Indoor Aerosols – Calculation of Zonal Particle Concentration and Particle Deposition in the Human Respiratory Tract

Jan DRZYMALLA*[1], Sebastian THEIßEN[1], Jannick HÖPER[1] and Andreas HENNE[1]

[1] TH Köln (University of Applied Sciences), Institute of Building Services Engineering, 50679 Cologne, Germany

* *Corresponding author: jan_stefan.drzymalla@th-koeln.de*

ABSTRACT

This study presents a modeling approach to calculate the particle concentration in mechanically conditioned indoor environments and predict particle deposition in the Human Respiratory Tract (HRT) by combining two aerosol models. The developed Indoor Aerosol Model (IAM) combines the semi-empirical Respiratory Deposition Model (RDM) presented by the International Commission on Radiological Protection (ICRP) in its publication 66/130 with a Material Balance Model (MBM). This enables the determination of total regional deposition fractions in the HRT for different particle diameters, subjects, levels of exertion or respiration types. These total regional deposition fractions are then incorporated into the MBM, which can be used to determine the number and mass of particles deposited in the HRT over a maximum period of 24 hours. Furthermore, the time history of the airborne particle concentration, as well as the surface loading and, in addition, the particle fate can be determined for well-mixed single zones.

INTRODUCTION

Pollutants, gases and aerosol particles enter the atmosphere every day and spread in the immediate environment of humans (Edwards et al., 2021). Basically, whenever a person breathes, aerosol particles are deposited in the Human Respiratory Tract (HRT), where they can cause harmful effects depending on their type, concentration and residence time (Riediker et al., 2019). Due to the fact that people usually spend more than 80% of their lives in enclosed indoor spaces (Błaszczyk et al., 2017; Matz et al., 2014), air quality, and thus aerosol concentration in buildings, plays a major role in health, well-being and comfort.

Indoor Air Quality (IAQ) is an important aspect in the design, construction, and operation of buildings. Especially engineers in the field of building services engineering aim to ensure a high IAQ for the future occupants already during the design phase of buildings (Spengler & Chen, 2000; Woods, 1991). For example, air ventilation concepts are developed, air handling systems are equipped with particle filters or low-polluting materials are used. In most cases, however, the design methods used are static and limited to regulatory or standardized minimum requirements. A dynamic pollutant assessment, as would be required for an aerosol simulation, is only carried out in a very few cases. The simulations and evaluations of deposited particles in the HRT, which go beyond this, are not in the design of buildings. The reasons for this are manifold. On the one hand, it is due to the fact that the engineers or project participants involved are not obliged to apply it and the financial aspects supposedly outweigh the benefits. On the other hand, a pollutant assessment can become very complex due to an insufficient database, varying boundary conditions or a lack of knowledge. Nevertheless, a pollutant assessment, especially an indoor aerosol modeling, can be of great benefit and also provide a huge improvement in IAQ.

Indoor particle concentrations are continuously determined by temporally but also spatially varying particle sources and sinks, which include, for example, equipment (e.g. printers), indoor activities, chemical transformation processes, deposition processes, air filtration, or even local particle concentrations in outdoor air (Morawska & Salthammer, 2003). Mathematical models can be used to balance these sources and sinks in order to predict or simulate the time history of particle concentration or other aspects of IAQ. The most popular IAQ models include the Material Balance Models (MBMs) (Hussein & Kulmala, 2008; Morawska & Salthammer, 2003; Nazaroff, 2004; Nazaroff & Cass, 1989; Thornburg et al., 2001) and Computational Fluid Dynamics (CFD) models (Fan, 1995). If these IAQ models are used to account for aerosols, they are referred to as Indoor Aerosol Models (IAMs) instead of IAQ models. Within the last decades numerous IAMs have been developed, which differ fundamentally in their application purpose, complexity as well as accuracy (Morawska & Salthammer, 2003). Even the current COVID-19 pandemic was and still is a real driver in the development of new and extension of existing IAMs (Dols et al., 2020; Jones et al., 2021; Kennedy et al., 2021). In addition, next to IAMs, there are various Respiratory Deposition Models (RDMs) that allow the calculation of regional deposition fractions in the HRT. Combining such a model with an IAM opens up a whole new range of prediction possibilities. For example, it would be possible to simulate a working day in an office and predict the amount of particles deposited in employees' HRTs. In the following, this study presents such a modeling approach, combining the semi-empirical RDM

presented by the International Commission on Radiological Protection (ICRP) in its publication 66/130 (International Commission on Radiological Protection [ICRP], 1994, 2015) with a MBM. Subsequently, the developed IAM is tested within the scope of a case study. The overall goal is to familiarize engineers and planners from the construction sector with the combined indoor aerosol modeling in order to ultimately improve IAQ.

METHODS

Material Balance Model

MBMs are based on the principle of particle number or mass conservation. These models apply to both a single zone and multiple zones, where a zone usually describes a room or a section of a room within a building (Morawska & Salthammer, 2003). They can be used to predict particle concentration levels and to assess other related parameters such as surface loadings. The present study uses a MBM for a single zone with continually operating Heating, Ventilation, and Air-Conditioning (HVAC) system, which is characterized by an uniform aerosol concentration (Dols et al., 2018; Dols et al., 2020) and shown schematically in Figure 1.

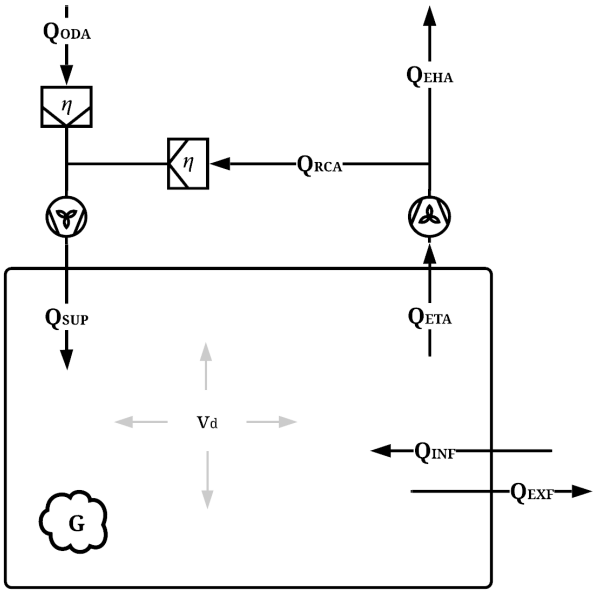

Figure 1. Schematic diagram of the single zone MBM

The MBM is based on a single, representative particle size of an aerosol to be simulated and assumes constant system parameters (e.g. airflow rates and filter efficiencies) during the period under consideration. Air can be supplied to and extracted from the zone under consideration of the existing HVAC system. The required supply (Q_{SUP}) and extract airflow rates (Q_{ETA}) as well as the associated outdoor air fraction ($\%_{ODA}$) must be defined as input parameters before the simulation starts. This in turn results in outdoor (Q_{ODA}), recirculation (Q_{RCA}) and exhaust airflow rates (Q_{EHA}). If the supply and extract airflow rates are equal, the zone is balanced. Otherwise, there is either negative or positive pressure, which affects the infiltration (Q_{INF}) and exfiltration rates (Q_{EXF}) through the zones envelope.

The mass balance for a single zone can be described by the following differential Equation (1) (Dols et al., 2018; Dols et al., 2020):

$$V\frac{dC_{IDA}}{dt} = PQ_{INF}C_{ODA}(t) + Q_{SUP}C_{SUP}(t) + G(t) - Q_{EXF}C_{IDA}(t) - Q_{ETA}C_{IDA}(t) - \sum_{i=1}^{N_s} v_{d,i}\,A_{s,i}C_{IDA}(t) \quad (1)$$

where V is the volume and C_{IDA} the particle concentration of the zone. The terms on the right-hand side of Equation (1) correspond to six different individual effects (Morawska & Salthammer, 2003). The first term corresponds to the effect of natural infiltration, where P describes the particle penetration coefficient and C_{ODA} the particle concentration of outdoor air. The second term corresponds to the air intake from the HVAC system, where C_{SUP} describes the particle concentration of supply air, which, taking Equation (2) into account, can be expressed according to Equation (3) (Nazaroff & Cass, 1989):

$$Q_{SUP} = Q_{ODA} + Q_{RCA} \quad (2)$$

$$C_{SUP}(t) = \frac{(1-\eta_{ODA})Q_{ODA}C_{ODA}(t)+(1-\eta_{RCA})Q_{RCA}C_{IDA}(t)}{Q_{ODA}+Q_{RCA}} \quad (3)$$

where η_{ODA} is the particle filtration efficiency of the outdoor air particle filter and η_{RCA} the particle filtration efficiency of the recirculation air particle filter. Term three on the right-hand side of Equation (1) corresponds to an indoor source G, also called particle generation rate, which accounts for indoor emissions or particles generated indoors (e.g. by occupants or equipment). In addition to the effect of infiltration, the mass balance also takes into account the effect of natural exfiltration, which is represented by the term four. Finally, term five corresponds to the mechanical ventilation out-take (extract air) and term six to the particle losses due to deposition on surfaces, where $v_{d,i}$ is the particle deposition velocity for surface i, $A_{s,i}$ the area for surface i and N_s the total number of surfaces. Taking Equations (2), (3) and (4) into account, the mass balance from Equation (1) can be transformed into Equation (5) which states that the time rate of change in mass of particles within the zone air is equal to the rate that particles are added and removed from the zone air (Dols et al., 2020):

$$Q_{EHA} = Q_{ETA} - Q_{RCA} \quad (4)$$

$$V\frac{dC_{IDA}}{dt} = C_{ODA}(t)(\mathrm{P}Q_{INF} + (1-\eta_{ODA})Q_{ODA}) + G(t) - C_{IDA}(t)(Q_{EXF} + Q_{EHA} + \eta_{RCA}Q_{RCA}) - \sum_{i=1}^{N_s} v_{d,i}\,A_{s,i}C_{IDA}(t) \quad (5).$$

In order to calculate the time history of the surface loading, the following differential Equation (6) must be set up (Dols et al., 2018):

$$A_{s,i}\frac{dL_{s,i}}{dt} = v_{d,i}A_{s,i}C_{IDA}(t) \quad (6)$$

where $L_{s,i}$ is the surface loading for surface i. Equation (6) indicates the time rate of change of particle mass on the surfaces of the zone is equal to the rate that particles are deposited on the surfaces (Dols et al., 2020).

Respiratory Deposition Model

Many mathematical models have been developed to predict total and regional particle deposition in the HRT (Hinds, 1999). An advanced and widely used model has been developed by the ICRP (ICRP, 1994).

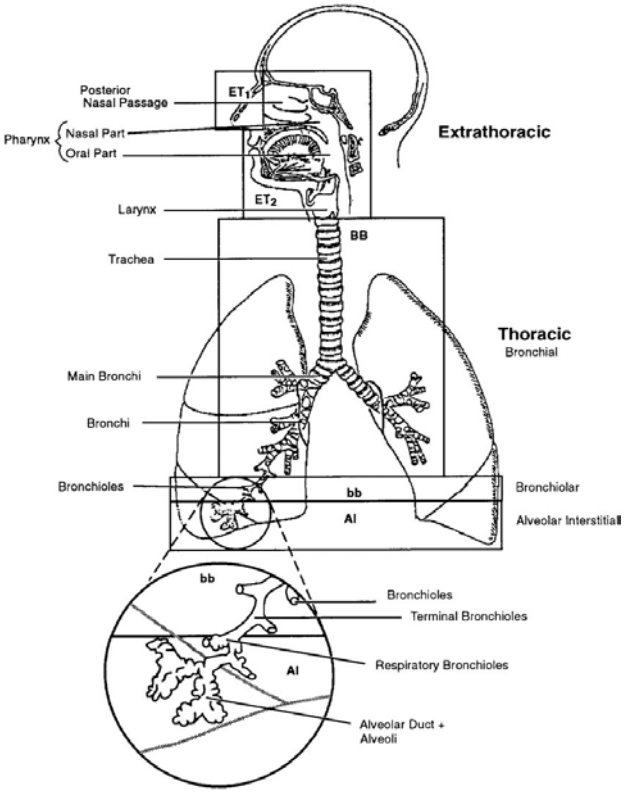

Figure 2. Respiratory tract regions defined in the RDM (ICRP, 2015)

This semi-empirical model uses equations based on experimental data and theory to characterize deposition by settling, inertia and diffusion in five regions of the respiratory system. These regions include the anterior nasal passages (ET1), naso-oropharynx and larynx (ET2), bronchi (BB), bronchioles (bb) and alveolar interstitium (AI) (ICRP, 1994) which are shown in Figure 2. Each mentioned region is represented by an equivalent particle filter that acts in series. As a result of each breath (inhalation and exhalation), particles are carried by a tidal airflow through each anatomical region or rather particle filter (see Figure 3).

For each region j (ET1 corresponds to j=1, ET2 to j=2, BB to j=3, bb to j=4 and AI to j=5), a total deposition fraction DF_j can be calculated, which sum up to the total respiratory deposition fraction DF_{Tot} in Equation (7) (Hinds, 1999; ICRP, 1994):

$$DF_{Tot} = \sum_{j=1}^{N=5} DF_j \qquad (7)$$

where N is the total number of respiratory tract regions.

For calculation purposes, it is comfortable to consider each region j, except AI, as having separate deposition fractions for inhalation ($DF_{j,inh}$) and exhalation ($DF_{j,ex}$). Consequently, regions 1 to 4 are passed through twice for each breath, resulting in a total number of regional filters in series of N_{ft}=9. For regions j=1 to 4, DF_j can be rewritten as:

$$DF_j = DF_{j,inh} + DF_{j,ex} = DE_j + DE_{N_{ft}-j+1} \qquad (8)$$

where DE_j is denoted hereafter as the deposition efficiency of regional filter j. For j=5, DF_j equals DE_j, because the AI is passed only once during a breathing cycle:

$$DF_j = DE_j \qquad (9).$$

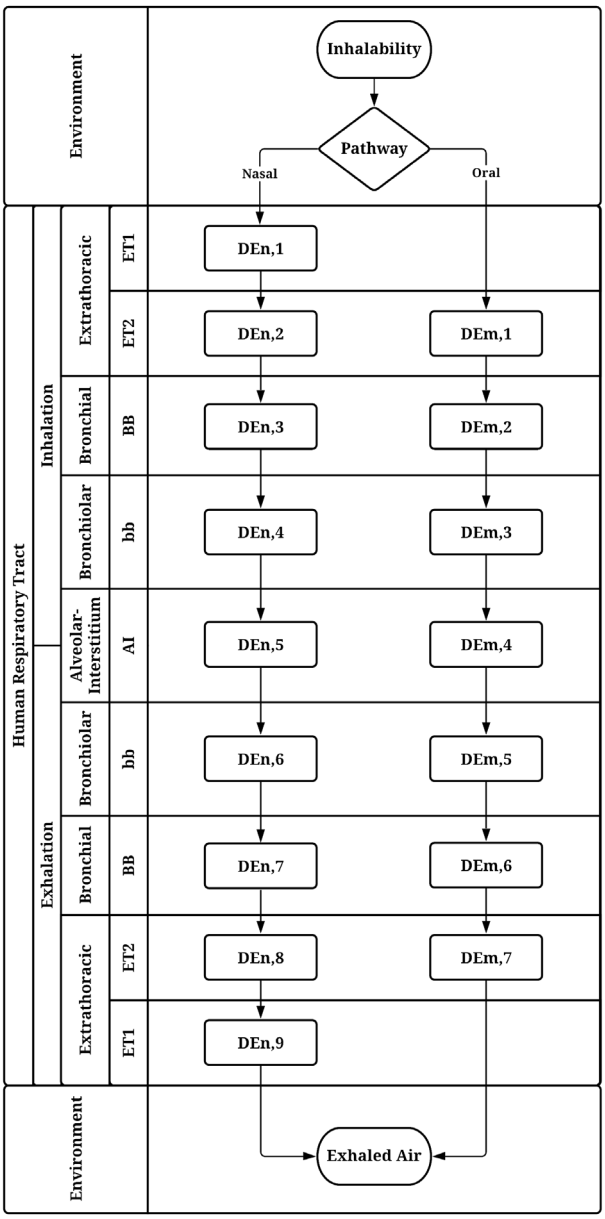

Figure 3. Schematic representation of inhalability of particles through nasal and oral pathway and their deposition in the anatomical regions during continuous cyclic breathing

Moreover, in addition to dividing inhalation and exhalation, it is useful to consider each region j, as having separate deposition efficiencies for the nasal and oral pathway.

When considering the nasal pathway, DE_j equals $DE_{ncor,j}$ as shown in Equation (10) and must be specified for the regional filters j=1 (Equation (11)), j=2 (Equation (12)), j=3 to 7 (Equation (13)) and j=8 to 9 (Equation (14)) (ICRP, 2015):

$$DE_j = DE_{ncor,j}, \quad \text{for } j=1,N_{ft} \tag{10}$$

$$DE_{ncor,j} = 0.65\begin{pmatrix}DE_{n,j} + DE_{n,j+1} + \\ DE_{n,j+7} + DE_{n,j+8}\end{pmatrix} \tag{11}$$

$$DE_{ncor,j} = 0.35\begin{pmatrix}DE_{n,j-1} + DE_{n,j} + \\ DE_{n,j+6} + DE_{n,j+7}\end{pmatrix} \tag{12}$$

$$DE_{ncor,j} = DE_{n,j} \tag{13}$$

$$DE_{ncor,j} = 0 \tag{14}$$

where $DE_{ncor,j}$ is the corrected and $DE_{n,j}$ the uncorrected deposition efficiency for the nasal pathway for regional filter j.

When considering the oral pathway, DE_j can be rewritten as Equation (15) (ICRP, 1994):

$$DE_j = f_n DE_{ncor,j} + (1 - f_n)DE_{m,j-1}, \quad \text{for } j=1,N_{ft} \tag{15}$$

where f_n is the fraction of total ventilatory airflow passing through the nose (see Table 1) and $DE_{m,j}$ is called the deposition efficiency for the oral pathway for regional filter j. It should be taken into account that the region ET1 is not passed during the oral pathway, which is the reason why $DE_{m,j-1}$ for j=1 and 9 does not exist respectively must equals zero.

Table 1. Fraction of total ventilatory airflow passing through the nose (f_n) (ICRP, 1994)

Level of exertion	Respiration type		Unit
	Nose breather	Mouth breather	
Sleep	1.00	0.70	-
Sitting	1.00	0.70	-
Light exercise	1.00	0.40	-
Heavy exercise	0.50	0.30	-

In order to calculate $DE_{n,j}$ and $DE_{m,j}$, Equation (16) can be used for regional filter j=1 by substituting the indices n (nose) and m (mouth) by k (ICRP, 1994):

$$DE_{k,j} = \eta_{k,j}\left(1 - \eta_{pre}\right) \tag{16}$$

where $\eta_{k,j}$ is the total filtration efficiency for nose or mouth breathing for regional filter j and η_{pre} is the intake efficiency or inhalability of the imaginary prefilter with which airborne particles are inspired into the HRT (Equation (23)). $\eta_{k,j}$ considers the aerodynamic deposition (e.g. impaction and gravitational settling) and thermodynamic deposition (e.g. diffusion by Brownian motion) processes and describes the combined filtration efficiency for regional filter j and can be calculated with Equation (17) (ICRP, 1994):

$$\eta_{k,j} = \left(\eta_{k,ae,j}^2 + \eta_{k,th,j}^2\right)^{0.5} \tag{17}$$

where $\eta_{k,ae,j}$ corresponds to the aerodynamic filtration efficiency for regional filter j during nasal or mouth breathing and can be easily calculated using the equations on Table 12 of ICRP publication 66 (ICRP, 1994) and the aerodynamic diameter d_{ae} (for $d_e < 0.002\ \mu m$ see Equation (22)). $\eta_{k,th,j}$ on the other hand corresponds to the thermodynamic filtration efficiency for regional filter j during nasal or mouth breathing and requires, next to the equations on table 13 of ICRP publication 66 (ICRP, 1994), a series of complex intermediate calculations. A key parameter for calculating $\eta_{k,th,j}$ is the diffusion coefficient D, which can be calculated according to Equation (18) (ICRP, 1994):

$$D = \frac{C(d_{th})k_B T}{3\pi\mu d_{th}} \tag{18}$$

where $C(d_{th})$ is the slip correction for a particle of thermodynamic diameter, k_B is Boltzmann's constant ($1.38{\cdot}10^{-16}$ erg·s·K^{-1}), T is the absolute temperature of the HRT (310.00 K), μ is the dynamic efficiency of air ($1.88{\cdot}10^{-4}$ erg·s·cm^{-3}) and d_{th} is the thermodynamic diameter.

Generally, the slip correction factors are given by substituting either d_{ae} or d_{th}, respectively for d_e (caution for $d_e < 0.002\ \mu m$) in Equation (19) (ICRP, 1994; Klumpp & Bertelli, 2017):

$$C(d_e) = 1 + \frac{76\lambda}{pd_e}\left(2.514 + 0.8e^{\left(-\frac{0.55pd_e}{76\lambda}\right)}\right) \tag{19}$$

where λ is the mean free path of the air molecules at 37.00 °C (0.0683 µm) (ICRP, 2002), 100% relative humidity and 76.00 cm·Hg atmospheric pressure p.

To calculate $C(d_{th})$, the thermodynamic diameter d_{th} is needed, which can be described as a function of d_{ae} which has to be solved recursively, by initially setting (ICRP, 1994):

$$d_{th,1} = d_{ae}\sqrt{\frac{X}{\rho}} \tag{20}$$

where X is the dynamic shape factor (ranges from 1 to 2) and ρ is the particle density. Then Equation (21) should be iterated for ii=2 to 21, whereby d_{th} converges for N_{it}=21 to the correct value ($d_{th} = d_{th,21}$) (ICRP, 1994; Klumpp & Bertelli, 2017):

$$d_{th,ii} = d_{ae}\sqrt{\frac{X\rho_0}{\rho}\frac{C(d_{ae})}{C(d_{th,ii-1})}} \tag{21}$$

where ρ_0 is the unity density (1.00 g·cm^{-3}) and $C(d_{ae})$ is the slip correction for a particle of aerodynamic diameter. If $d_{th,ii} < 0.002\ \mu m$, a correction is needed defined by Equation (22) (ICRP, 1994):

$$d_e = d_{e,un}\left(1 + 3e^{\left(-2200d_{e,un}\right)}\right) \tag{22}$$

where $d_{e,un}$ is the uncorrected value of the particle diameter of interest (e.g. d_{th} or d_{ae}).

With the converged value of d_{th}, it is possible to calculate $C(d_{th})$, D and finally $\eta_{k,j}$. For the determination of $DE_{k,1}$, the calculation of η_{pre} is additionally necessary and expressed by Equation (23), taking Equation (24) into account (ICRP, 1994):

$$\eta_{pre} = (1 - \eta_I) \tag{23}$$

$$\eta_I = 1 - 0.5(1 - (7.6 \cdot 10^{-4} d_{ae}^{2.8} + 1)^{-1}) + 1 \cdot 10^{-5} U^{2.75} e^{(0.055 d_{ae})} \tag{24}$$

where η_I represents the particle inhalability and U the wind speed or inhalation velocity (default value of 1.00 m·s^{-1}).

By setting:

$$N_{ft} = 9, \text{for } k = n \tag{25}$$

$$N_{ft} = 7, \text{for } k = m \tag{26}$$

$DE_{k,j}$ can be calculated for the remaining regional filter stages using Equation (27) (ICRP, 1994):

$$DE_{k,j} = DE_{k,j-1} \eta_{k,j} \frac{\phi_{k,j}}{\phi_{k,j-1}} \left(\frac{1}{\eta_{k,j-1}} - 1 \right), \text{for } j=2, N_{ft} \tag{27}$$

where $\phi_{k,j}$ is the volumetric fraction for regional filter j for nasal or mouth breathing, which also can be calculated using equations on tables 12 and 13 of ICRP publication 66 (ICRP, 1994).

Combined Indoor Aerosol Model

A combination of the described MBM and the RDM enables an IAM for assessment of exposure and deposited particle quantity in the HRT. The combined IAM is based on Equation (5) and can be expressed as follows:

$$V \frac{dC_{IDA}}{dt} = C_{ODA}(t)(\mathrm{P} Q_{INF} + (1 - \eta_{ODA}) Q_{ODA}) + G(t) - C_{IDA}(t)(Q_{EXF} + Q_{EHA} + \eta_{RCA} Q_{RCA} + BDF_{Tot}) - \sum_{i=1}^{N_s} v_{d,i} A_{s,i} C_{IDA}(t) \tag{28}$$

taking DF_{Tot} and the ventilation or breathing rate B of the exposed subject of interest (see Table 2) into account. The term BDF_{Tot} describes the particle deposition in the HRT and is to be treated as a particle sink.

Table 2. Ventilation rate of the exposed subject (B) (ICRP, 1994)

Level of exertion	Subject		Unit
	Male	Female	
Sleep	0.45	0.32	m^3·h^{-1}
Sitting	0.54	0.39	m^3·h^{-1}
Light exercise	1.50	1.25	m^3·h^{-1}
Heavy exercise	3.00	2.70	m^3·h^{-1}

By setting:

$$C_{IDA} = C_{in}, \text{at t} = 0 \tag{29}$$

$$C_{IDA} = C_f, \text{for t} \to \infty \tag{30}$$

and integrating the differential Equation (28) gives (Morawska & Salthammer, 2003):

$$C_{IDA}(t) = (C_{in} - C_f) e^{(-Kt)} + C_f \tag{31}$$

$$C_f = \frac{C_{ODA}(\mathrm{P} Q_{INF} + (1 - \eta_{ODA}) Q_{ODA}) + G}{Q_{EXF} + Q_{EHA} + \eta_{RCA} Q_{RCA} + BDF_{Tot} + \sum_{i=1}^{N_s} v_{d,i} A_{s,i}} \tag{32}$$

$$K = \frac{Q_{EXF} + Q_{EHA} + \eta_{RCA} Q_{RCA} + BDF_{Tot} + \sum_{i=1}^{N_s} v_{d,i} A_{s,i}}{V} \tag{33}$$

where C_{in} is the initial zone concentration, C_f is the steady-state zone concentration, K is the total loss rate and t is the time step of interest. In order to calculate the surface loading, Equation (6) must also be integrated (Poppendieck, 2020):

$$L_{s,i}(t) = v_{d,i} \left(\begin{array}{c} \frac{C_{in}}{K} \left(1 - e^{(-Kt)}\right) + \\ C_f \left(t - \frac{1}{K} \left(1 - e^{(-Kt)}\right) \right) \end{array} \right) \tag{34}$$

The resulting IAM is applied in the following step.

CASE STUDY

To illustrate the application of the combined IAM presented in this study, the time history of the airborne particle concentration as well as the surface loading and, in addition, the particle fate for a mechanically ventilated single office room (see Figure 1) is simulated over a period of 24 hours. The simulation is carried out with the specially developed tool IAM$_{dep}$, which is based on Microsoft Excel. The considered office room has a floor area of $A_{s,fl}$=20.00 m^2 and a clear room height of H=3.00 m, resulting in a room volume of V=60.00 m^3, which corresponds to a representative single office (DIN V 18599:2018). The supply airflow rate is Q_{SUP}=80.00 m^3·h^{-1} (with $\%_{ODA}$=80.00%) and the extract airflow rate is Q_{ETA}=100.00 m^3·h^{-1}, resulting in a negative flow imbalance and thus an infiltration airflow rate of Q_{INF}=20.00 m^3·h^{-1}. Within the 24-hour period under consideration, the office is occupied from 07:00 to 18:00 by a healthy adult male who performs a light exercise (B=1.50 m^3·h^{-1}). Typically, it can be expected that, especially during the occupancy period, particles are generated indoors or resuspended, e.g. by the person present. In the context of this case study, it is assumed that no particles are generated indoors during the entire simulation period (G=0.00 #·h^{-1}), although the combined IAM could take these indoor emissions into account. This assumption is deliberately chosen to graphically highlight the deposition effect in the HRT and to avoid overlap with indoor sources (see Results). Besides, at the beginning of the simulation (t=0), there should be no airborne particles (C_{in}=0.00 #·m^{-3}) or particles on the surfaces ($L_{in,s,i}$=0.00 #·m^{-2}). The simulation is based on a single aerodynamic particle size of d_{ae}=1.00 µm with a particle density of ρ=1.00 g·cm^{-3} and represents a monodispersed aerosol to be simulated. The particle deposition velocity for

upward facing surfaces (floor) is assumed to be $v_{d,fl}$=3.50E-05 m·s^{-1} and for vertical surfaces (walls) $v_{d,w}$=1.00E-06 m·s^{-1} and can be neglected for downward facing surfaces (ceiling). These particle deposition velocities can be derived for a friction velocity of 0.10 m·s^{-1} from a deposition velocity model developed for deposition onto smooth surfaces as a function of friction velocity (K. Lai & Nazaroff, 2000). Moreover, the existing HVAC system has two particle filter that can trap particles from the outdoor and recirculation air. A particle number concentration of C_{ODA}=3.97865E+05 #·m^{-3} is assumed for the outdoor air, based on the sample particle size distribution as shown in Figure 4. The outdoor air particle filter has a filter efficiency of η_{ODA}=18.00% (corresponds to MERV 6) and the recirculation air particle filter a has filter efficiency of η_{RCA}=32.00% (corresponds to MERV 8) for particles with a diameter of 1.00 µm. In addition, a typical particle penetration coefficient of P=0.60 is assumed, indicating that 40.00% of the particles cannot infiltrate through the building envelope (Long et al., 2001; Thornburg et al., 2001). Furthermore, constant system parameters and a well-mixed indoor air are assumed for the simulation.

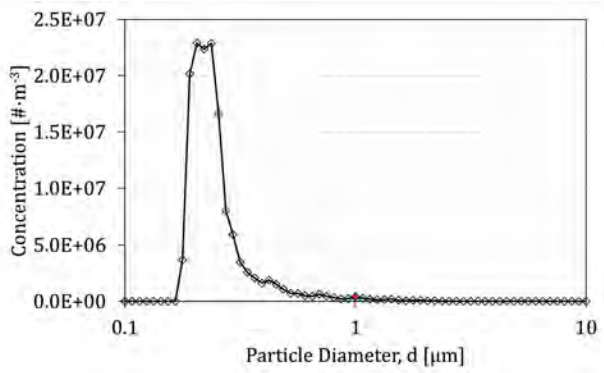

Figure 4. A sample particle size distribution (dC_{ODA}/dlog(d)) of the outdoor air (red marks the concentration for d=1 µm)

RESULTS AND DISCUSSION

With the help of the methods described in this study, an indoor aerosol modeling was carried out for the case study described above, the results of which are presented and discussed below. Figure 5 shows the time history of the airborne particle number concentration for the simulated office over a period of 24 hours and thus enables prediction of the IAQ or allows recommendations for action to be made. A distinction is made between the indoor concentration development over the entire simulation period (dashed curve) and the indoor concentration development during occupancy (solid curve). Looking at the entire simulation period (dashed curve), it is recognizable that the indoor concentration rises sharply at the beginning and reaches its peak after nearly four hours at approximately 2.79E+05 #·m^{-3}. Moreover, over the simulation period of 24 hours, an average concentration of 2.71E+05 #·m^{-3} or an average number of 1.62E+07 particles is obtained. Although the

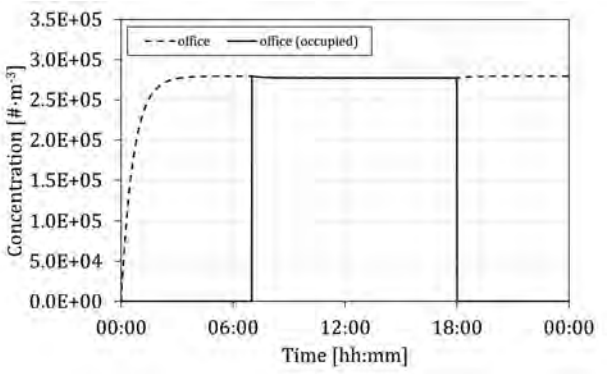

Figure 5. Simulated airborne particle number concentration (C_{IDA}) for d_{ae}=1.00 µm

indoor concentration converges to the outdoor concentration (C_{ODA}=3.97865E+05 #·m^{-3}) over time, but does not reach it, which has several reasons.On the one hand, the polluted outdoor air is drawn in by the HVAC system with an airflow rate of Q_{ODA}=64.00 m^3·h^{-1}, mixed with the recirculation airflow rate of Q_{RCA}=16.00 m^3·h^{-1} and only then continuously supplied into the office as mixed air with Q_{SUP}=80.00 m^3·h^{-1}. On the other hand, the existing particle filters trap particles from the outdoor and recirculation air and ensure a reduced supply air concentration. Throughout the entire simulation period, the outdoor air particle filter traps 1.44E+08 particles, corresponding to a particle mass of 7.56E+01 µg (see Table 3).

Table 3. Calculated particle fate

Particle fate	Particle number	Particle mass	Percentage
[-]	[#]	[µg]	[%]
Exited Office	5.46E+08	2.86E+02	65.25
Filtered from outdoor air	1.44E+08	7.56E+01	17.27
Filtered from recirculation air	3.33E+07	1.74E+01	3.98
Filtered via building envelope	7.64E+07	4.00E+01	9.14
Deposited on surfaces	1.76E+07	9.21E+00	2.10
Remain airborne	1.68E+07	8.78E+00	2.00
Deposited in HRT	2.17E+06	1.14E+00	0.26
Total	8.36E+08	4.38E+02	100.00

This in turn means that approximately 17.27% of the simulated particles are trapped by the outdoor air particle filter. The recirculation air particle filter, in contrast, traps 3.33E+07 particles, which corresponds to a particle mass of 1.74E+01 µg and accounts for approximately 3.98% of the simulated particles. Furthermore, the particles are deposited on the surfaces over time. As shown in Figure 6, surface loading increases linearly with time, where 92.84% of the depositing particles sediment to the floor and 7.16% settle on the walls. This is also a reason why the

maximum indoor particle concentration of 2.79E+05 #·m^{-3} is not exceeded. In relation to the overall context, however, the effect of particle deposition on surfaces accounts only for 2.10%. It should be noted that the simulation assumed an unfurnished room, and thus a smaller deposition surface area than probably exists in reality.

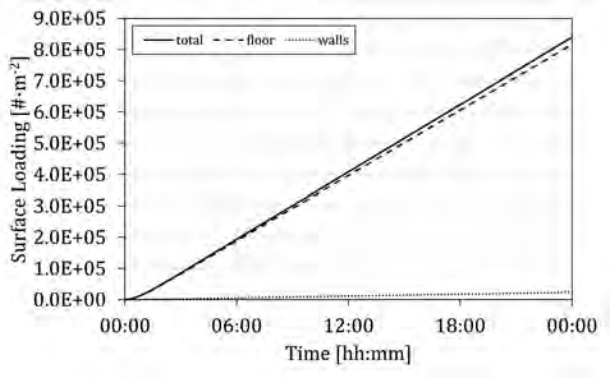

Figure 6. Simulated surface loads ($L_{s,i}$) for d_{ae}=1.00 µm

The cumulative surface loads and deposited particle numbers can be taken from Table 4 below.

Table 4. Cumulative surface loading results

Surface area i	Concentration	Particle number
[-]	[#·m^{-2}]	[#]
Floor	8.16E+05	1.63E+07
Walls	2.33E+04	1.26E+06
Total	8.40E+05	1.76E+07

Simultaneously 65.25% of the simulated particles are extracted out of the office with an airflow rate of Q_{ETA}=100.00 m^3·h^{-1}. As a result of the fact that more air is extracted than is supplied, a negative flow imbalance and thus an infiltration airflow rate of Q_{INF}=20.00 m^3·h^{-1} occurs. This leads to particles from the outdoor air infiltrating the office through the building envelope. Typically, 60.00% of the particles in the outdoor air with a diameter of 1.00 µm infiltrate through the building envelope, providing there is an infiltration airflow rate (Long et al., 2001; Thornburg et al., 2001). In this case, the building envelope traps 7.64E+07 particles, which corresponds to 9.14% of the simulated particles.

The combined IAM allows, in addition to the prediction of airborne particle concentration and surface loading, also an estimation of the particles deposited in the HRT. In the first step, the total regional deposition fractions (DF_j) must be determined with the help of the RDM. The calculated total deposition fractions of the regions ET1, ET2, BB, bb and AI can be taken from Table 5. A closer look at the deposition fractions reveals that about 47.00% of the total inhaled particles are deposited in the HRT. In relation to this total respiratory deposition fraction, 48.00% of the inhaled particles deposited in ET1, 25.85% in ET2, 2.12% in BB, 1.71% in bb and 22.32% in AI. This percentage distribution depends largely on the particle size (d_{ae}=1 µm), the level of exertion (light exercise, B=1.50m^3·h^{-1}) and the respiration type (nose breather). Once the deposition fractions are known, they can be integrated into the MBM in a second step, ultimately producing the combined IAM.

Looking at the simulation period during which the office is occupied (see Figure 5, solid curve), it can be seen that from the time of occupancy (07:00), the indoor concentration drops minimally and reaches a steady-state concentration of 2.77E+05 #·m^{-3}. In contrast, after the time of occupancy (18:00), the indoor concentration rises again to 2.79E+05 #·m^{-3}. It is therefore evident that a part of the airborne particles are inhaled, deposited in the HRT and finally lead to the temporary reduction of the indoor concentration. Specifically, 2.17E+06 particles were deposited in the HRT during the 11-hour occupancy period, which corresponds to a mass of 1.14E+00 µg (see Table 5). Compared to the other particle fates, 0.26% of the simulated particles were deposited in the HRT. However, this effect can be seen well, among other reasons, because it was assumed that the considered person does not emit any new particles, as is normally the case (Asadi et al., 2019).

Table 5. Calculated total regional deposition fractions (DF_j) and simulated deposited particle quantities in the HRT

Respiratory region j	Total regional deposition fraction (DF_j)	Deposited particle number (in HRT)	Deposited particle mass (in HRT)
[-]	[-]	[#]	[µg]
ET1	2.28E-01	1.04E+06	5.45E-01
ET2	1.23E-01	5.61E+05	2.94E-01
BB	1.01E-02	4.60E+04	2.41E-02
bb	8.10E-03	3.70E+04	1.94E-02
AI	1.06E-01	4.84E+05	2.53E-01
Total	4.74E-01	2.17E+06	1.14E+00

It must be noted that the methods presented and used have limitations. Only a single particle size can be modeled per simulation, which means that polydisperse aerosols can only be modeled indirectly by multiple simulation. Apart from this, chemical conversion processes or effects such as particle nucleation, coagulation or deactivation are not taken into account. Furthermore, a well-mixed single zone and constant system parameters (e.g. outdoor air concentration, air flow rates, filtration efficiencies, level of exertion, breathing rate or number of persons) must be assumed, which in reality can vary and be time-dependent. In addition, some input parameters (e.g. particle deposition velocities, inhalation velocity, initial surface loads or generation rate) have to be estimated, as they can only be determined correctly with great effort.

Based on the results of the case study, it could be shown that the modeling approach described in this study is very applicable and can be helpful for the estimation and evaluation of aerosol concentration development in indoors and aerosol deposition in the HRT. For example, in practice, engineers or planners

might consider different scenarios comparing different particle filters, airflow rates, particle sizes, or levels of exertion. In turn, this improves IAQ, benefits human health and also creates planning security.

CONCLUSIONS

The modeling approach presented is intended to help engineers or planners design buildings to reduce aerosol concentrations in offices, residential buildings, retail stores, education institutions or hospital rooms, ultimately improving IAQ. To ensure that the approach is actually applied in planning practice, project developers, building owners or investors must be convinced of the added value of such pollutant assessments. They finance construction projects and pass on their wishes and specifications to the engineers and planners, which are responsible for successful implementation. In meantime, however, awareness of healthy buildings is growing (e.g. COVID-19) and will also be demanded on an international level in the future (EU Technical Expert Group on Sustainable Finance [TEG], 2020).

However, there is a lack of information on the physical-chemical properties and emission rates of aerosol particles produced in indoor and outdoor environments (Hussein et al., 2015), which makes the IAM difficult to apply. Accordingly, further research is needed to obtain more information and benchmarks on indoor sources and their emission factors. Nevertheless, the combined IAM represents a promising solution approach that may complement or replace experimental investigations.

Finally, to ensure that the combined IAM developed does not represent an isolated solution in the future, the authors propose standardizing the calculation processes described. As a holistic and cooperative working method, Building Information Modeling (BIM) is the ideal solution for process improvement and standardization in the design of buildings. Within the BIM method, the non-proprietary open source data format Industry Foundation Classes (IFC) is used, which offers interfaces beyond software boundaries that allow the exchange of information between different disciplines on the basis of a BIM model. With the help of the IFC extension schema, the BIM model created e.g. by the architect could consequently be enriched with aerosol-specific information. For example, information on emission rates, particle size distributions, occupancy or information about the existing HVAC system (e.g. airflow rates or filter efficiencies) could be added to the BIM model. In contrast to the previous aerosol assessment, the necessary information are thus available earlier, in a more structured and uniform manner and can be directly linked to the building or zone. Based on this, calculation processes could be automated, thus facilitating the application.

NOMENCLATURE

$A_{s,i}$ = deposition surface area for surface i (m^2)

$A_{s,fl}$ = deposition surface area for upward facing surfaces (floor) (m^2)

B = breathing rate ($m^3 \cdot s^{-1}$)

C_f = steady-state concentration ($\# \cdot m^{-3}$)

C_{IDA} = indoor particle concentration ($\# \cdot m^{-3}$)

C_{in} = initial indoor particle concentration ($\# \cdot m^{-3}$)

C_{ODA} = outdoor particle concentration ($\# \cdot m^{-3}$)

C_{SUP} = particle concentration in supply air ($\# \cdot m^{-3}$)

$C(d_e)$ = slip correction for particle diameter d_e (µm)

$C(d_{ae})$ = slip correction for particle diameter d_{ae} (µm)

$C(d_{th})$ = slip correction for particle diameter d_{th} (µm)

D = particle diffusion coefficient ($cm^2 \cdot s^{-1}$)

d = particle diameter (µm)

d_{ae} = aerodynamic particle diameter (µm)

d_e = equivalent particle diameter of interest (µm)

$d_{e,un}$ = uncorrected equivalent particle diameter of interest (µm)

d_{th} = thermodynamic particle diameter (µm)

$d_{th,ii}$ = thermodynamic particle diameter for iteration step ii (µm)

DE_j = deposition efficiency for regional filter j (-)

$DE_{k,j}$ = deposition efficiency for regional filter j during nasal or mouth breathing (-)

$DE_{m,j}$ = deposition efficiency for the oral pathway for regional filter j (-)

$DE_{n,j}$ = uncorrected deposition efficiency for the nasal pathway for regional filter j (-)

$DE_{ncor,j}$ = corrected deposition efficiency for the nasal pathway for regional filter j (-)

DF_j = total deposition fraction for region j (-)

$DF_{j,ex}$ = deposition fraction for exhalation and region j (-)

$DF_{j,inh}$ = deposition fraction for inhalation and region j (-)

DF_{Tot} = total respiratory deposition fraction (-)

f_n = fraction of total ventilatory airflow passing through the nose (-)

G = particle generation rate ($\# \cdot s^{-1}$)

H = clear room height (m)

K = total loss rate (s^{-1})

k_B = boltzmann's constant ($1.38 \cdot 10^{-16}$ erg·s·K^{-1})

$L_{s,i}$ = surface loading for surface i ($\# \cdot m^{-2}$)

$L_{in,s,i}$ = initial surface loading for surface i ($\# \cdot m^{-2}$)

N = total number of respiratory tract regions (-)

N_s = total number of surfaces (-)

N_{ft} = total number of regional filters in series (-)

N_{it} = total number of iteration steps (-)

P = particle penetration coefficient (-)

p = atmospheric pressure (cm·Hg)

Q_{EHA} = exhaust airflow rate ($m^3 \cdot s^{-1}$)

Q_{ETA} = extract airflow rate ($m^3 \cdot s^{-1}$)

Q_{EXF} = exfiltration airflow rate ($m^3 \cdot s^{-1}$)

Q_{INF} = infiltration airflow rate ($m^3 \cdot s^{-1}$)

Q_{ODA} = outdoor airflow rate ($m^3 \cdot s^{-1}$)

Q_{RCA} = recirculation airflow rate ($m^3 \cdot s^{-1}$)

Q_{SUP} = supply airflow rate ($m^3 \cdot s^{-1}$)

T = absolute temperature of the respiratory tract (310.00 K)

t = time (s)

U = the wind speed or inhalation velocity (default value of 1.00 $m \cdot s^{-1}$)

V = volume (m^3)

$v_{d,i}$ = particle deposition velocity for surface i ($m \cdot s^{-1}$)

$v_{d,fl}$ = particle deposition velocity for upward facing surfaces (floor) ($m \cdot s^{-1}$)

$v_{d,w}$ = particle deposition velocity for vertical surfaces (walls) ($m \cdot s^{-1}$)

X = particle shape factor which ranges between 1.00 to 2.00 (-)

$\%_{ODA}$ = outdoor air fraction (-)

η_I = inhalability of particles (-)

$\eta_{k,j}$ = total filtration efficiency for regional filter j during nasal or mouth breathing (-)

$\eta_{k,ae,j}$ = aerodynamic filtration efficiency for regional filter j during nasal or mouth breathing (-)

$\eta_{k,th,j}$ = thermodynamic filtration efficiency for regional filter j during nasal or mouth breathing (-)

η_{ODA} = particle filtration efficiency of the outdoor air particle filter (-)

η_{pre} = intake efficiency or inhalability of the imaginary prefilter with which airborne particles are inspired into the respiratory tract (-)

η_{RCA} = particle filtration efficiency of the recirculation air particle filter (-)

μ = dynamic efficiency of air ($1.88 \cdot 10^{-4}$ erg·s·cm^{-3})

ρ = particle density ($g \cdot cm^{-3}$)

ρ_0 = unity density (1.00 $g \cdot cm^{-3}$)

λ = mean free path of the air molecules at 37.00 °C (0.0683 µm)

$\phi_{k,j}$ = volumetric fraction for regional filter j during nasal or mouth breathing

REFERENCES

Asadi, S., Wexler, A. S., Cappa, C. D., Barreda, S., Bouvier, N. M., & Ristenpart, W. D. (2019). "Aerosol emission and superemission during human speech increase with voice loudness". *Scientific Reports*, *9*(1), 1-10. https://doi.org/10.1038/s41598-019-38808-z

Błaszczyk, E., Rogula-Kozłowska, W., Klejnowski, K., Kubiesa, P., Fulara, I., & Mielżyńska-Švach, D. (2017). "Indoor air quality in urban and rural kindergartens: Short-term studies in Silesia", Poland. *Air Quality, Atmosphere & Health*, *10*(10), 1207–1220. https://doi.org/10.1007/s11869-017-0505-9

Deutsches Institut für Normung e. V. (2018). *Energetische Bewertung von Gebäuden - Berechnung des Nutz-, End- und Primärenergiebedarfs für Heizung, Kühlung, Lüftung, Trinkwarmwasser und Beleuchtung - Teil 10: Nutzungsrandbedingungen, Klimadaten* (DIN V 18599-10).

Dols, W. S., Persily, A. K., & Polidoro, B. J. (2018). *Development of Airborne Nanoparticle Exposure Modeling Tools* (NIST Technical Note No. 2004). Gaithersburg, MD USA. https://doi.org/10.6028/NIST.TN.2004

Dols, W. S., Polidoro, B. J., Poppendieck, D. G., & Emmerich, S. J. (2020). *A Tool to Model the Fate and Transport of Indoor Microbiological Aerosols (FaTIMA)* (NIST Technical Note No. 2095). Gaithersburg, MD USA. https://doi.org/10.6028/NIST.TN.2095

Edwards, D. A., Ausiello, D., Salzman, J., Devlin, T., Langer, R., Beddingfield, B. J., Fears, A. C., Doyle-Meyers, L. A., Redmann, R. K., Killeen, S. Z., Maness, N. J., & Roy, C. J. (2021). "Exhaled aerosol increases with COVID-19 infection, age, and obesity". *Proceedings of the National Academy of Sciences of the United States of America*, *118*(8). https://doi.org/10.1073/pnas.2021830118

EU Technical Expert Group on Sustainable Finance. (2020). *Taxonomy Report: Technical Annex*.

Fan, Y. (1995). "CFD modelling of the air and contaminant distribution in rooms". *Energy and Buildings*, *23*(1), 33–39. https://doi.org/10.1016/0378-7788(95)00916-L

Hinds, W. C. (1999). *Aerosol Technology: Properties, Behavior, and Measurement of Airborne Particles* (2 end.). John Wiley & Sons.

Hussein, T., & Kulmala, M. (2008). "Indoor Aerosol Modeling: Basic Principles and Practical Applications". *Water, Air, & Soil Pollution: Focus*, *8*(1), 23–34. https://doi.org/10.1007/s11267-007-9134-x

Hussein, T., Wierzbicka, A., Löndahl, J., Lazaridis, M., & Hänninen, O. (2015). "Indoor aerosol modeling for assessment of exposure and respiratory tract deposited dose". *Atmospheric Environment*, *106*, 402–411. https://doi.org/10.1016/j.atmosenv.2014.07.034

International Commission on Radiological Protection. (1994). *Human Respiratory Tract Model for Radiological Protection* (1st ed.). *ICRP publication: Vol. 66*. Pergamon.

International Commission on Radiological Protection (2002). "ERRATA FOR PUBLICATIONS 66, 68, 69, 71, 72, and 78". *Annals of the ICRP*, *32*(1-2), 307–312. https://doi.org/10.1016/S0146-6453(02)00027-1

International Commission on Radiological Protection (2015). "Icrp Publication 130: Occupational Intakes of Radionuclides: Part 1". *Annals of the ICRP*, *44*(2), 5–188. https://doi.org/10.1177/0146645315577539

Jones, B., Sharpe, P., Iddon, C., Hathway, E. A., Noakes, C. J., & Fitzgerald, S. (2021). "Modelling uncertainty in the relative risk of exposure to the SARS-CoV-2 virus by airborne aerosol transmission in well mixed indoor air". *Building and Environment*, *191*, 107617. https://doi.org/10.1016/j.buildenv.2021.107617

K. Lai, A. C., & Nazaroff, W. W. (2000). "MODELING INDOOR PARTICLE DEPOSITION FROM TURBULENT FLOW ONTO SMOOTH SURFACES". *Journal of Aerosol Science*, *31*(4), 463–476. https://doi.org/10.1016/S0021-8502(99)00536-4

Kennedy, M., Lee, S. J., & Epstein, M. (2021). "Modeling aerosol transmission of SARS-CoV-2 in multi-room facility". *Journal of Loss Prevention in the Process Industries*, *69*, 104336. https://doi.org/10.1016/j.jlp.2020.104336

Klumpp, J., & Bertelli, L. (2017). "Kdep: A Resource for Calculating Particle Deposition in the Respiratory Tract". *Health Physics*, *113*(2), 110–121. https://doi.org/10.1097/HP.0000000000000679

Long, C. M., Suh, H. H., Catalano, P. J., & Koutrakis, P. (2001). "Using time- and size-resolved particulate data to quantify indoor penetration and deposition behavior". *Environmental Science & Technology*, *35*(10), 2089–2099. https://doi.org/10.1021/es001477d

Matz, C. J., Stieb, D. M., Davis, K., Egyed, M., Rose, A., Chou, B., & Brion, O. (2014). "Effects of age, season, gender and urban-rural status on time-activity: Canadianhuman Activity Pattern Survey 2 (CHAPS 2) ". *International Journal of Environmental Research and Public Health*, *11*(2), 2108–2124. https://doi.org/10.3390/ijerph110202108

Morawska, L., & Salthammer, T. (2003). *Indoor Environment: Airborne Particles and Settled Dust*. Wiley-VCH.

Nazaroff, W. W. (2004). "Indoor Particle Dynamics". *Indoor Air*, *14 Suppl 7*, 175–183. https://doi.org/10.1111/j.1600-0668.2004.00286.x

Nazaroff, W. W., & Cass, G. R. (1989). "Mathematical Modeling of Indoor Aerosol Dynamics". *Environmental Science & Technology*, *23*(2), 157–166. https://doi.org/10.1021/es00179a003

Poppendieck, D. (2020). *Tool for Evaluation of Vaporized Hydrogen Peroxide Disinfection of N95 Masks in Small Rooms* (NIST Technical Note No. 2091). Gaithersburg, MD. https://doi.org/10.6028/NIST.TN.2091

Riediker, M., Zink, D., Kreyling, W., Oberdörster, G., Elder, A., Graham, U., Lynch, I., Duschl, A., Ichihara, G., Ichihara, S., Kobayashi, T., Hisanaga, N., Umezawa, M., Cheng, T.-J., Handy, R., Gulumian, M., Tinkle, S., & Cassee, F. (2019). "Particle toxicology and health - where are we?". *Particle and Fibre Toxicology*, *16*(1), 19. https://doi.org/10.1186/s12989-019-0302-8

Spengler, J. D., & Chen, Q. (2000). "Indoor Air Quality Factors in Designing a Healthy Building". *Annual Review of Energy and the Environment*, *25*(1), 567–600. https://doi.org/10.1146/annurev.energy.25.1.567

Thornburg, J., Ensor, D. S., Rodes, C. E., Lawless, P. A., Sparks, L. E., & Mosley, R. B. (2001). "Penetration of Particles into Buildings and Associated Physical Factors. Part I: Model Development and Computer Simulations". *Aerosol Science and Technology*, *34*(3), 284–296. https://doi.org/10.1080/02786820119886

Woods, J. E. (1991). "An Engineering Approach to Controlling Indoor Air Quality". *Environmental Health Perspectives*, *95*, 15–21. https://doi.org/10.1289/ehp.919515